Journal of Solid Mechanics Vol. 11, No. 2 (2019) pp. 454-474
DOI: 10.22034/JSM.2019.665912

Vibration, Buckling and Deflection Analysis of Cracked Thin Magneto Electro Elastic Plate Under Thermal Environment

Shashank Soni [1,*], N. K. Jain [1], P. V. Joshi [2]

[1] *National Institute of Technology, Raipur, Chhattisgarh, India*
[2] *Department of Basic Sciences and Engineering, Indian Institute of Information Technology, Nagpur, India*

Received 25 March 2019; accepted 20 May 2019

ABSTRACT

The Magneto-Electro-Elastic (MEE) material exhibits pyroelectric and pyromagnetic effects under thermal environment. The effects of such pyroelectric and pyromagnetic behavior on vibration, buckling and deflection analysis of partially cracked thin MEE plate is presented and discussed in this paper. The aim of the study is to develop an analytical model for the vibration and geometrically linear thermal buckling analysis of cracked MEE plate based on the classical plate theory (CPT). The line spring model (LSM) is modified for the crack terms to accommodate the effect of electric and magnetic field rigidities, whereas the effect of thermal environment is accommodated in the form of thermal moment and in-plane forces. A classical relation for thermal buckling phenomenon of cracked MEE plate is also proposed. The governing equation for cracked MEE plate has also been solved to get central deflection which shows an important phenomenon of shift in primary resonance due to crack and temperature rise. The results evaluated for natural frequencies as affected by crack length, plate aspect ratio and critical buckling temperature are presented for first four modes of vibration. The obtained results reveal that the fundamental frequency of the cracked plate decreases with increase in temperature and crack length. Furthermore the variation of the critical buckling temperature with plate aspect ratio and crack length is also established for different modes of vibration.

Keywords : Vibration; Buckling; Temperature; Crack; Magneto-electro-elastic plate.

1 INTRODUCTION

MAGNETO-ELECTRO-ELASTIC materials belong to the family of smart materials; they exhibit interaction between elastic, electro-magnetic effects and have ability to convert energy among electricity, elasticity and magnetism. Such behavior of MEE material has widespread opportunities to devise efficient sensors and actuators for smart structures [1]. MEE thin plates are widely used in electric packaging, electromagnetic

[*] Corresponding author. Tel.: +91 9098417902.
E-mail address: shashanksoninitr@gmail.com (Shashank Soni).

probes, ultrasonic imaging, acoustics, actuators and sensors [1–3]. In the past decade, various analytical and numerical approaches have been proposed for the vibration analysis of smart structures. Among them, the systematic investigations for determining dynamic characteristics and material properties of the MEE plates have drawn significant attention of researches by different authors. Chen et al. [4] determined the effective properties of $BaTiO_3$–$CoFe_2O_4$ layered composite and established a model for the linear coupling effect between electricity, elasticity and magnetism of the MEE composite. The effective magneto-electro-elastic moduli of fiber reinforced and laminated $BaTiO_3$–$CoFe_2O_4$ composite is determined by Li [5]. They concluded for both fibrous and laminated composite the variation in the volume fraction of $BaTiO_3$ affects the magneto-electro coefficients. Xue and Pan [6] calculated the effective Poisson's ratio and Young's modulus of the MEE composite rod made of different volume fraction of $BaTiO_3$ material in $BaTiO_3$ - $CoFe_2O_4$ composite. Wu and Huang [7] presented an analytical approach for investigating the effective material properties of fibrous MEE composite using and the Mori-Tanaka theory. In absence of thermal environment, Pan [8] derived a three dimensional exact solution for anisotropic MEE rectangular plate with all edges simply supported, under both surface and internal loads. Then, extending their previous work Pan and Heyliger [9] derived an analytical solution for free vibration analysis of the multilayered MEE composite plate under simply supported boundary condition. Ramirez et al., [10,11] presented an analytical solution for free vibration problem of MEE plates and determined vibration characteristics of laminated MEE plates [10] and Functionally graded MEE composite plates [11]. Moita et al., [12] presented a higher order FEM model for the static and free vibration analysis of laminated MEE plate. Liu and Chang [3] proposed a closed form expression for the vibration analysis of thin MEE composite plate. They evaluated the natural frequency analytically for different volume fraction of piezoelectric material $BaTiO_3$ using the classical plate theory. Similarly, the studies vibration problems of laminated MEE intact plates using single-layer approach has also been proposed by different researchers [13–16]. Li and Zhang [17] used Mindlin plate theory to derive the equation of motion for vibration problem of a magneto-electro-elastic plate resting on a Pasternak foundation. Liu [2] determined the exact solution for deformation analysis for fiber reinforced MEE composite plate and derived a closed form expression for the vibration problem of MEE plate using Kirchhoff thin-plate theory. Similarly, many researchers (Ref. [18–20]) investigated vibration of multilayered MEE plates using the FSDT and classical theory. Phoenix et al. [21] proposed mathematical formulation for the static and dynamic analysis of coupled magneto-electro-elastic problems using finite element method. They worked on the coupled magneto-electro-elastic problems using extended RMVT theorem. Guan and He [22] obtained the analytical solution of governing equation for 2D problem of transversely isotropic MEE plate by simplifying the physical quantities in form of four harmonic functions using Almansi's theorem. Recently, Shooshtari and Razavi [23] used higher-order theory (HSDT) for vibration problems of intact MEE plates and they also proposed a mathematical model for it. With the thermal effects considered, Rao and Sunar [24] studied the influence of temperature variation on overall performance of a distributed control system made of piezoelectric material. Li and Dunn [25] and Li [26] also included the thermal effects in their proposed formulation to study the effective behavior of MEE composite under thermal environment. Using the displacement and stress functions. Chen et al., [27] proposed an analytical solution for free vibration problem of transversely isotropic magneto-electro-thermo-elastic plate using the potential theory method. Recently, Hou et al. [28,29] investigated a 3-D Green's function for a steady point heat source on the surface of a semi-infinite and two-phase transversely isotropic magneto-electro-thermo-elastic material by Chen's general solution. Ke [30] studied the vibration response of MEE nano-plates using the nonlocal and Kirchhoff plate theory under influence of thermal environment. It is known that the cracks or holes in a plate make its dynamic behavior drastically different from that of an intact plate. Mostly numerical techniques are used for static solutions for cracked plate, but an approximate analytical solution has been proposed by the simplified Line Spring Model (LSM). This concept was first introduced by Rice and Levy [31], for investigating the analytical solution of cracked plates based on Kirchhoff's thin plate theory. They represented the surface crack as persistent line spring with stretching, bending and twisting compliances. Later on the effect of transverse shear deformation is also introduced in the model by Delalae and Erdogan [32] to improve the effectiveness of model. Zheng and Dai [33] determined the stress intensity factors at the crack tips by employing this simplified LSM of cracked isotopic plate. Khadem and Rezaee [34] were introduced the modified comparison functions for analysis of a simply supported cracked rectangular plate. Using the LSM, an approximate analytical model for an isotropic thin rectangular plate with a part-through surface crack located at its centre was first time developed by Israr et al. [35]. They were expressed the relationship between tensile and bending force effects at far sides of the plate and at crack location in their work. By extending the work of Israr et al. [35], Ismail and Cartmell [36] developed an analytical model for cracked rectangular plate with various angular orientation of crack and they validated their results with experimentation also. It is concluded from their work that the increase in length of crack and its angular orientation decreases the natural frequencies of plate. Recently, Joshi et al. [37,38] and Gupta et al. [39,40] have also extended the work of Israr et al. [35] for multiple line cracks located at the centre of the cracked

isotropic [37,39] and orthotropic plates [38,40]. They modified the developed model of Israr et al. [35] to incorporate the influence of internal cracks in it. Extending their work, the analysis on vibration and buckling problems of partially cracked isotropic [41] and orthotropic plates [42] under influence of thermal environment has been also presented by them. Soni et al. [43] performed an analytical study on non linear vibration problem of cracked MEE plate submerged in fluid. They modified the previously developed models to accommodate the effect of fluidic medium. The literature shows that the vibration of intact plates is affected by the presence of thermal environment and the work of researchers (Refs.[37,38,41,42]) show that the vibration of plates is affected by the presence of crack. Thus the study of influence of crack on the vibration behavior of magneto-electro-thermo-elastic plates becomes significant. As per the author's knowledge, there seems no study dealing with the modeling of the vibration problem of partially cracked magneto-electro-elastic plates in thermal environment. The difficulty in coupling the elasticity, electricity, magnetism and pyroeffects under thermal environment may be the reason. The present study fills this gap by proposing an analytical model which addresses the following:

1. Modeling of free vibrations of partially cracked magneto-electro-elastic plates considering the effect of thermal environment.
2. A unique classical relation for critical buckling temperature of cracked magneto-electro-elastic plate is presented considering the pyroelectric and pyromagnetic behavior of the plate.
3. The classical relation for central deflection of cracked MEE plate which shows an important phenomenon of shift in primary resonance due to crack and temperature rise.
4. New results are presented for fundamental frequencies of cracked magneto-electro-elastic plate as affected by crack length, plate aspect ratio and rise in temperature.
5. The coupling effect of elasticity, electricity, temperature and magnetism has been incorporated in the constitutive relations.

The present work extends the analytical model proposed by Joshi et al. [41,42] and applies it to the case of a transversely isotropic cracked MEE plate in the presence of thermal environment, The MEE plate material is made of fiber-reinforced $BaTiO_3$–$CoFe_2O_4$ composite, contains a partial crack at the centre of plate. The simplified LSM for elasticity is modified to accommodate the pyroelectric and pyromagnetic behavior of MEE plate. The influence of thermal environment is incorporated by considering thermal moments and in-plane forces due to temperature. The in-plane deflections are assumed to be restricted either by boundary conditions or by adjacent structures in both x and y directions. The plate configuration is shown in Fig. 1 in which the dimensions of the plate taken along x and y directions are l_1 and l_2 respectively. The thickness of the plate is represented by h. 2a is the crack length at plate centre which is parallel to the x axis and the depth of the crack is assumed to be constant. The simply supported boundary condition (SSSS) shown in Fig. 2 is considered to study the effect of crack length, plate aspect ratio and critical buckling temperature on the vibration response of magneto-electro-thermo-elastic plate.

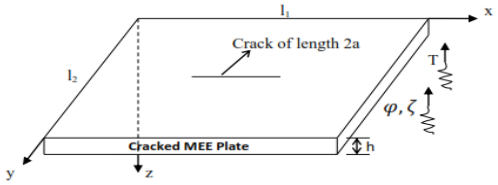

Fig.1
Plate configuration showing a part through surface crack at the center of plate.

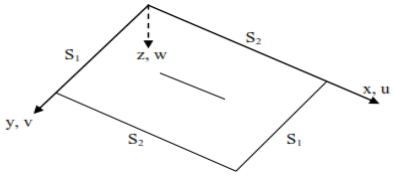

$$S_1 \rightarrow u = w = M_x = N_{Txy} = 0$$
$$S_2 \rightarrow v = w = M_y = N_{Tyx} = 0$$

Fig.2
Cracked MEE plate with all edges simply supported and in-plane displacements restricted.

2 GOVERNING EQUATION

For the MEE plate, it is known that the equation of motion based on the Kirchhoff's classical plate hypothesis represents the effect of electricity and magnetism in plate by the electrical and magnetic field rigidities. To

incorporate the effect of thermal environment for a thin MEE rectangular plate, the pyroelectric and pyromagnetic coefficients are considered in the stress-strain relations. To derive such a governing equation of motion for partially cracked magneto-electro-thermo-elastic plate as shown in Fig. 1, the following assumptions are adopted for modeling;

1. The plate is presumed as thin, homogenous and impeccably elastic composed of Magneto-electro-elastic material.
2. The mid-plane stays unstrained consequent to bending, for that reason the normal strain (ε_z), resulting from transverse loading, might be discarded. The normal stress σ_z is neglected from constitutive relations in the modeling because of small magnitude as compared to the other stress components.
3. Effects of rotary inertia and shear deformation are neglected.
4. The temperature variation is thought to be linear all through the thickness of the plate; $T(z) = T_{avg} + ((\Delta T)z)/2$, where $\Delta T = T_t - T_b$ is the temperature difference between the top and the bottom surface of the plate and $T_{avg} = (T_t + T_b)/2$ is average temperature.

Consider a transversely isotropic magneto-electro-thermo-elastic plate in Cartesian coordinates with *z* direction along the plate thickness and perpendicular to the plane of isotropy. Based on the above classical assumptions, the constitutive relations for magneto-electro-thermo-elastic plate can be obtained [3,44–46],[43]as:

$$\begin{aligned}
\sigma_x &= \tilde{c}_{11}\varepsilon_x + \tilde{c}_{12}\varepsilon_y + \tilde{e}_{31}\varphi_{,z} + q_{31}\zeta_{,z} + \beta_1 T(z) \\
\sigma_y &= \tilde{c}_{12}\varepsilon_x + \tilde{c}_{11}\varepsilon_y + \tilde{e}_{31}\varphi_{,z} + q_{31}\zeta_{,z} + \beta_2 T(z) \\
\tau_{xy} &= \tilde{c}_{66}\gamma_{xy} = \tilde{c}_{66}(\varepsilon_x + \varepsilon_y)
\end{aligned} \tag{1}$$

$$D_z = \tilde{e}_{31}\varepsilon_x + \tilde{e}_{31}\varepsilon_y - E_{33}\varphi_{,z} - d_{33}\zeta_{,z} - P_3 T(z) \tag{2}$$

$$D_z = \tilde{e}_{31}\varepsilon_x + \tilde{e}_{31}\varepsilon_y - E_{33}\varphi_{,z} - d_{33}\zeta_{,z} - P_3 T(z) \tag{3}$$

where

$$\begin{aligned}
&\tilde{c}_{11} = c_{11} - c_{13}c_{13}/c_{33} && \tilde{c}_{12} = c_{12} - c_{13}c_{13}/c_{33} && \tilde{e}_{31} = e_{31} - c_{13}e_{33}/c_{33} && q_{31} = q_{31} - c_{13}q_{33}/c_{33} \\
&E_{33} = E_{33} + e_{33}e_{33}/c_{33} && \mu_{33} = \mu_{33} + q_{33}q_{33}/c_{33} && d_{33} = d_{33} + e_{33}q_{33}/c_{33} && \tilde{c}_{66} = c_{66} \\
&\beta_1 = \beta_2 = \beta_1 - c_{13}\beta_3/c_{33} && P_3 = P_3 + e_{33}\beta_3/c_{33} && \tilde{\tau}_3 = \tau_3 + q_{33}\beta_3/c_{33}
\end{aligned}$$

σ_x, σ_y , and $\varepsilon_x, \varepsilon_y$ are the normal stresses and normal strains in *x* and *y* direction respectively. Similarly, γ_{xy} and τ_{xy} are the strain and shear stress of *x*-*y* plane. ζ, φ and $T(z)$ are the magnetic potential, electric potential and temperature increment respectively. B_i and D_i are magnetic induction and electric displacement components. c_{ij}, e_{ij}, E_{ij}, d_{ij}, q_{ij}, μ_{ij}, β_i, P_i and τ_i are the elastic, piezoelectric, dielectric, magnetoelectric, piezomagnetic, magnetic, thermal modulus, pyroelectric and pyromagnetic constants respectively. In present work, all type material constants are assumed to be constant. In the absence of the electric charge, body force and current, the equilibrium equations can be expressed as:

$$\begin{aligned}
\frac{\partial \sigma_x}{\partial x} + \frac{\partial \tau_{xy}}{\partial y} + \frac{\partial \tau_{xz}}{\partial z} &= 0 \\
\frac{\partial \tau_{xy}}{\partial x} + \frac{\partial \sigma_y}{\partial y} + \frac{\partial \tau_{yz}}{\partial z} &= 0 \\
\frac{\partial \tau_{xz}}{\partial x} + \frac{\partial \tau_{yz}}{\partial y} + \frac{\partial \sigma_z}{\partial z} &= 0
\end{aligned} \tag{4}$$

$$\frac{\partial D_x}{\partial x}+\frac{\partial D_y}{\partial y}+\frac{\partial D_z}{\partial z}=0 \tag{5}$$

$$\frac{\partial B_x}{\partial x}+\frac{\partial B_y}{\partial y}+\frac{\partial B_z}{\partial z}=0 \tag{6}$$

On substituting Eqs.(2) and (3) into Eqs.(5) and (6) respectively, one can express the two equations (Eqs. (5) and (6)) as:

$$E_{33}\varphi_{,zz}+d_{33}\zeta_{,zz}=\tilde{e}_{31}\frac{\partial(\varepsilon_x+\varepsilon_y)}{\partial z}-P_3\frac{\partial T(z)}{\partial z} \tag{7}$$

$$d_{33}\varphi_{,zz}+\mu_{33}\zeta_{,zz}=q_{31}\frac{\partial(\varepsilon_x+\varepsilon_y)}{\partial z}-\tilde{\tau}_3\frac{\partial T(z)}{\partial z} \tag{8}$$

which also implies,

$$E_{33}\frac{\partial^2\varphi}{\partial z^2}+d_{33}\frac{\partial^2\zeta}{\partial z^2}=\tilde{e}_{31}\frac{\partial(\varepsilon_x+\varepsilon_y)}{\partial z}-P_3\frac{\partial T(z)}{\partial z} \tag{9}$$

$$d_{33}\frac{\partial^2\varphi}{\partial z^2}+\mu_{33}\frac{\partial^2\zeta}{\partial z^2}=q_{31}\frac{\partial(\varepsilon_x+\varepsilon_y)}{\partial z}-\tilde{\tau}_3\frac{\partial T(z)}{\partial z} \tag{10}$$

On solving Eq. (9) and Eq. (10) using crammer's rule of determinants, one obtains;

$$\frac{\partial^2\varphi}{\partial z^2}=\frac{\Delta_1}{\Delta}\frac{\partial(\varepsilon_x+\varepsilon_y)}{\partial z}-\frac{\Delta_3}{\Delta}\frac{\partial T(z)}{\partial z} \tag{11}$$

$$\frac{\partial^2\zeta}{\partial z^2}=\frac{\Delta_2}{\Delta}\frac{\partial(\varepsilon_x+\varepsilon_y)}{\partial z}-\frac{\Delta_4}{\Delta}\frac{\partial T(z)}{\partial z} \tag{12}$$

where

$$\Delta=E_{33}\mu_{33}-d_{33}^2 \qquad \Delta_1=\tilde{e}_{31}\mu_{33}-d_{33}q_{31} \qquad \Delta_2=E_{33}q_{31}-d_{33}\tilde{e}_{31} \qquad \Delta_3=P_3\mu_{33}-\tilde{\tau}_3 d_{33} \qquad \Delta_4=\tilde{\tau}_3 E_{33}-P_3 d_{33}$$

Integration of Eqs.(11) and (12) yields,

$$\varphi_{,z}=\frac{\partial\varphi}{\partial z}=\frac{\Delta_1}{\Delta}\left(\varepsilon_x+\varepsilon_y\right)-\frac{\Delta_3}{\Delta}T(z)+\varphi_0$$
$$\zeta_{,z}=\frac{\partial\zeta}{\partial z}=\frac{\Delta_2}{\Delta}\left(\varepsilon_x+\varepsilon_y\right)-\frac{\Delta_4}{\Delta}T(z)+\zeta_0$$

where, φ_0 and ζ_0 are the integration constants also can be treated as the variation of electric and magnetic field in the transverse direction of plate. In present work closed-circuit magneto-electric boundary condition is considered implying that, these constants, φ_0 and ζ_0 can be taken as zero [23]. Hence the above two expressions of electric and magnetic potential can be simplified to,

$$\varphi_{,z}=\frac{\partial\varphi}{\partial z}=\frac{\Delta_1}{\Delta}\left(\varepsilon_x+\varepsilon_y\right)-\frac{\Delta_3}{\Delta}T(z) \tag{13}$$

$$\zeta_{,z} = \frac{\partial \zeta}{\partial z} = \frac{\Delta_2}{\Delta}\left(\varepsilon_x + \varepsilon_y\right) - \frac{\Delta_4}{\Delta} T(z) \tag{14}$$

Eq.(13) and Eq.(14) represents the variation of electric and magnetic potential along the plate thickness direction in terms of normal strains in plane directions. On representing the mid surface strains (ε_x ,ε_y and γ_{xy}) in terms of lateral deflection as:

$$\varepsilon_x = -z\,\frac{\partial^2 w}{\partial x^2} \qquad \varepsilon_y = -z\,\frac{\partial^2 w}{\partial y^2} \qquad \gamma_{xy} = -2z\,\frac{\partial^2 w}{\partial x\,\partial y} \tag{15}$$

On substituting Eqs. (13) – (15) in Eq.(1), one can obtain the bending moments in terms of lateral deflection as:

$$M_x = \int_{-\frac{h}{2}}^{+\frac{h}{2}} \sigma_x z dz = M_{xe} + M_{xele} + M_{xm} + M_{Tx} \tag{16}$$

$$M_y = \int_{-\frac{h}{2}}^{+\frac{h}{2}} \sigma_y z dz = M_{ye} + M_{yele} + M_{ym} + M_{Ty} \tag{17}$$

$$M_{xy} = \int_{-\frac{h}{2}}^{+\frac{h}{2}} \tau_{xy} z dz = -\frac{h^3}{12}\left[2\tilde{c}_{66}\frac{\partial^2 w}{\partial x\,\partial y}\right] \tag{18}$$

where, $M_{xe} = -\frac{h^3}{12}\left[\tilde{c}_{11}\frac{\partial^2 w}{\partial x^2} + \tilde{c}_{12}\frac{\partial^2 w}{\partial y^2}\right]$ and $M_{ye} = -\frac{h^3}{12}\left[\tilde{c}_{12}\frac{\partial^2 w}{\partial x^2} + \tilde{c}_{11}\frac{\partial^2 w}{\partial y^2}\right]$ are the moments due to elasticity. $M_{xele} = M_{yele} = -\frac{h^3}{12}\left[\tilde{e}_{31}\frac{\Delta_1}{\Delta}\nabla^2 w\right]$ are the moments due to electric field. $M_{xm} = M_{ym} = -\frac{h^3}{12}\left[q_{31}\frac{\Delta_2}{\Delta}\nabla^2 w\right]$ are the moments due to magnetic field. $M_{Tx} = M_{Ty} = \left(\beta_1 - \tilde{e}_{31}\frac{\Delta_3}{\Delta} - q_{31}\frac{\Delta_4}{\Delta}\right)\int_{-\frac{h}{2}}^{+\frac{h}{2}} T(z) z dz$ are the resultant thermal moment due to thermal environment.

Consider a cracked MEE plate element having all the bending moments and transverse forces acting on the mid-plane as shown in Fig. 3. Apart from the elastic bending moments, the bending moments due to electric field (M_{xele} ,M_{yele}), magnetic field (M_{xm} ,M_{ym}) and temperature (M_{Tx} ,M_{Ty}) is also shown in Fig. 3. m_y is the additional bending moment due to the crack of length 2a which represents the effect of crack as deduced in line spring model (LSM). Use of such additional bending moment (m_y) for a surface crack of length 2a is also evident in the published work of Israr et al. [35].

On taking the equilibrium of all the forces along *z* direction, one obtains,

$$\frac{\partial Q_x}{\partial x} + \frac{\partial Q_y}{\partial y} = \rho h\,\frac{\partial^2 w}{\partial t^2} - P_z \tag{19}$$

where, Q_x and Q_y are the transverse forces per unit length in the plate thickness direction, $\rho h\,\frac{\partial^2 w}{\partial t^2}$ represents the inertia force of vibrating plate in which ρ is the density and *h* is the thickness of plate and P_z is the transverse load per unit area.

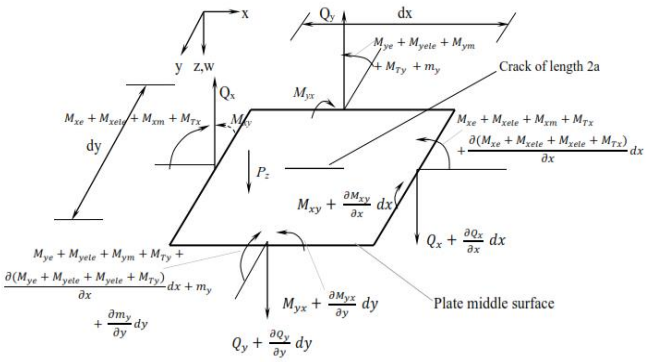

Fig.3
Plate element showing bending moments and transverse forces on middle plane.

On taking moment about the *x* and *y* axes, the equilibrium equations can be written as:

$$\sum M_x = 0;\ \frac{\partial M_{ye}}{\partial y} + \frac{\partial M_{yele}}{\partial y} + \frac{\partial M_{ym}}{\partial y} + \frac{\partial M_{Ty}}{\partial y} + \frac{\partial m_y}{\partial y} + \frac{\partial M_{xy}}{\partial x} = Q_y \tag{20}$$

$$\sum M_y = 0;\ \frac{\partial M_{xe}}{\partial x} + \frac{\partial M_{xele}}{\partial x} + \frac{\partial M_{xm}}{\partial x} + \frac{\partial M_{Tx}}{\partial x} + \frac{\partial M_{yx}}{\partial y} = Q_x \tag{21}$$

Employing Eq.(20) and (21) in Eq.(19) one obtains,

$$\frac{\partial^2 M_{xe}}{\partial x^2} + \frac{\partial^2 M_{xele}}{\partial x^2} + \frac{\partial^2 M_{xm}}{\partial x^2} + \frac{\partial^2 M_{Tx}}{\partial x^2} + \frac{\partial^2 M_{ye}}{\partial y^2} + \frac{\partial^2 M_{yele}}{\partial y^2} + \frac{\partial^2 M_{ym}}{\partial y^2} + \frac{\partial^2 M_{Ty}}{\partial y^2} + \frac{\partial^2 m_y}{\partial y^2} + \frac{\partial^2 M_{xy}}{\partial x\,\partial y} + \frac{\partial^2 M_{yx}}{\partial x\,\partial y} = \rho h \frac{\partial^2 w}{\partial t^2} - P_z \tag{22}$$

On substituting the bending moments in terms of lateral deflection from Eqs. (16) – (18) into Eq.(22), the governing equation for cracked MEE plate can be given as:

$$\frac{h^3}{12}\left\{\tilde{c}_{11}\left(\frac{\partial^4 w}{\partial x^4} + \frac{\partial^4 w}{\partial y^4}\right) + 2\left(\tilde{c}_{12} + 2\tilde{c}_{66}\right)\frac{\partial^4 w}{\partial x^2 \partial y^2} + \tilde{e}_{31}\frac{\Delta_1}{\Delta}\nabla^4 w + q_{31}\frac{\Delta_2}{\Delta}\nabla^4 w\right\} = -\rho h \frac{\partial^2 w}{\partial t^2} + \frac{\partial^2 M_{Tx}}{\partial x^2} + \frac{\partial^2 M_{Ty}}{\partial y^2} + \frac{\partial^2 m_y}{\partial y^2} + P_z \tag{23}$$

Since the relation $\tilde{c}_{11} = \tilde{c}_{12} + 2\tilde{c}_{66}$ holds [3] for any transversely isotropic material therefore Eq.(23) can be simplified as:

$$\frac{h^3}{12}\left\{\tilde{c}_{11}\nabla^4 w + \tilde{e}_{31}\frac{\Delta_1}{\Delta}\nabla^4 w + q_{31}\frac{\Delta_2}{\Delta}\nabla^4 w\right\} = -\rho h \frac{\partial^2 w}{\partial t^2} + \frac{\partial^2 M_{Tx}}{\partial x^2} + \frac{\partial^2 M_{Ty}}{\partial y^2} + \frac{\partial^2 m_y}{\partial y^2} + P_z \tag{24}$$

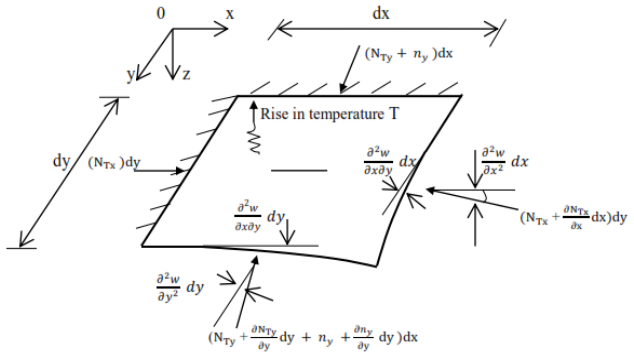

Fig.4
In-plane forces on a plate element due to thermal environment and crack of length 2*a*.

with the in-plane displacements in both *x* and *y* direction being restricted, the uniform or non uniform heating of the cracked plate causes membrane or in-plane forces [35,37,41,42,47]. Literature (Refs. [35,37,38]) show the addition of such in-plane forces to the governing differential equation of motion. The application of magneto-electro-thermo-elastic thin plates in actuators and sensors are generally subjected to in-plane forces either by plate boundary conditions or adjacent structures or temperature variation. In the present study for magneto-electro-thermo-elastic plates, the in-plane forces only due to temperature variation (N_{Tx} and N_{Ty}) are considered and in-plane forces due to stretching (N_x, N_y and N_{xy}) are neglected as they do not affect the stiffness of plate. To consider these thermal in-plane forces for the cracked MEE plate, it is arbitrarily assumed in CCFF boundary condition which means the two adjacent edges of the plate are fixed and the other two free. Other boundary conditions are equally treatable. Fig. 4 shows the equilibrium of in-plane forces on the cracked plate. n_y is the additional in-plane force due to crack. Taking equilibrium of in-plane forces along *z* axis leads to,

$$\sum F_z = -N_{Tx}\frac{\partial^2 w}{\partial x^2} - N_{Ty}\frac{\partial^2 w}{\partial y^2} - n_y\frac{\partial^2 w}{\partial y^2} \tag{25}$$

where N_{Tx} and N_{Ty} are the in-plane forces per unit length due to the temperature variation and n_y is the additional in-plane force per unit length due to the crack of length 2a (Ref. [41]). The shear force N_{Txy} is neglected in Fig. 4 as temperature does not affect the shear component [48][49]. On adding the in-plane forces of Eq.(25) to Eq. (24), the final governing equation of a cracked MEE plate becomes;

$$\frac{h^3}{12}\left\{c_{11}\nabla^4 w + e_{31}\frac{\Delta_1}{\Delta}\nabla^4 w + q_{31}\frac{\Delta_2}{\Delta}\nabla^4 w\right\} = -\rho h\frac{\partial^2 w}{\partial t^2} + \frac{\partial^2 M_{Tx}}{\partial x^2} + \frac{\partial^2 M_{Ty}}{\partial y^2}$$
$$+\frac{\partial^2 m_y}{\partial y^2} - N_{Tx}\frac{\partial^2 w}{\partial x^2} - N_{Ty}\frac{\partial^2 w}{\partial y^2} - n_y\frac{\partial^2 w}{\partial y^2} + P_z$$

or

$$\left\{D\nabla^4 w + E\nabla^4 w + M\nabla^4 w\right\} = -\rho h\frac{\partial^2 w}{\partial t^2} + \frac{\partial^2 M_{Tx}}{\partial x^2} + \frac{\partial^2 M_{Ty}}{\partial y^2} + \frac{\partial^2 m_y}{\partial y^2} - N_{Tx}\frac{\partial^2 w}{\partial x^2} - N_{Ty}\frac{\partial^2 w}{\partial y^2} - n_y\frac{\partial^2 w}{\partial y^2} + P_z \tag{26}$$

where, $D = \tilde{c}_{11}\frac{h^3}{12}$ represents the elastic rigidity, $E = \tilde{e}_{31}\frac{h^3}{12}\frac{\Delta_1}{\Delta}$ and $M = q_{31}\frac{h^3}{12}\frac{\Delta_2}{\Delta}$ denotes the effective rigidities due to electricity and magnetism respectively.

Literature on the study of cracked plates shows that many of the researchers used the line spring model to formulate the crack terms for additional bending moment (m_y) and in-plane force (n_y). It gives the relationship between the bending and tensile stresses at the crack location and at far sides of the plate. Recently, Joshi et al. [41] and Soni et al. [43] derived the above relationship of the tensile and bending loads at the far sides of the plate and at the crack location in presence of thermal environment for the isotropic and MEE plates. Thus the relations for resultant in-plane forces n_y and bending moments m_y can be written as [41] [43],

$$n_y = \frac{2a}{\left(6\delta_{bt} + \delta_{tt}\right)\left(1-\nu^2\right)h + 2a}N_{Ty} \tag{27}$$

$$m_y = -\frac{2a}{3\left(\frac{\delta_{bt}}{6} + \delta_{bb}\right)(3+\nu)(1-\nu)h + 2a}\left(M_{ye} + M_{yele} + M_{ym} + M_{Ty}\right) \tag{28}$$

where, the terms δ_{bb} ,δ_{tt} ,$\delta_{bt}=\delta_{tb}$ are crack compliance coefficients for bending, stretching and tensile-bending respectively. The crack compliance coefficients depend on crack depth (*d*) to thickness (*h*) ratio and vanish when $d=0$. The required expressions for compliance coefficients as a function of the ratio of crack depth to plate thickness $(\delta=d/h)$ can be written as (Ref. [35]),

$$\delta_{tt}=1.154\delta^2\left[1.98-0.54\delta^1+18.65\delta^2-33.70\delta^3+99.26\delta^4-211.90\delta^5+436.84\delta^6-460.48\delta^7+289.98\delta^8\right]$$
$$\delta_{bb}=1.154\delta^2\left[1.98-3.28\delta^1+14.43\delta^2-31.26\delta^3+63.56\delta^4-103.36\delta^5+147.52\delta^6-127.69\delta^7+61.50\delta^8\right]$$
$$\delta_{bt}=\alpha_{tb}=1.154\delta^2\left[1.98-1.91\delta^1+16.01\delta^2-34.84\delta^3+83.93\delta^4-153.65\delta^5+256.72\delta^6-244.67\delta^7+133.55\delta^8\right]$$

It is noted that these above expressions for compliance coefficients are valid only for $(\delta=d/h)$ values within the range 0.1– 0.7 and in the present model these δ is taken 0.6. *v* is the effective Poisson's ratio of MEE plate and it can be expressed as (Ref. [6]),

$$\nu=\frac{q_{33}q_{31}+\mu_{33}c_{13}+\left[\left(d_{33}q_{31}-e_{31}\mu_{33}\right)\left(e_{33}\mu_{33}-d_{33}q_{33}\right)/\left(d_{33}^2-E_{33}\mu_{33}\right)\right]}{2q_{31}^2+\mu_{33}\left(c_{11}+c_{12}\right)+\left[2\left(d_{33}q_{31}-e_{31}\mu_{33}\right)\left(e_{33}\mu_{33}-d_{33}q_{33}\right)/\left(d_{33}^2-E_{33}\mu_{33}\right)\right]}$$

On employing Eq. (27) and (28) in Eq. (26) and expressing the moment M_y in terms of transverse deflection (w) from Eq. (17) we get the required governing equation of cracked MEE plate as:

$$\left\{D\nabla^4w+E\nabla^4w+M\nabla^4w\right\}=-\rho h\frac{\partial^2w}{\partial t^2}+\frac{\partial^2M_{Tx}}{\partial x^2}+\frac{\partial^2M_{Ty}}{\partial y^2}-N_{Tx}\frac{\partial^2w}{\partial x^2}-N_{Ty}\frac{\partial^2w}{\partial y^2}$$
$$-\frac{2a}{3\left(\frac{\delta_{bt}}{6}+\delta_{bb}\right)\left(3+\nu\right)\left(1-\nu\right)h+2a}\frac{\partial^2\left(M_{ye}+M_{yele}+M_{ym}+M_{Ty}\right)}{\partial y^2}-\frac{2a}{\left(6\delta_{bt}+\delta_{tt}\right)\left(1-\nu^2\right)h+2a}N_{Ty}\frac{\partial^2w}{\partial y^2}+P_z \tag{29}$$

Similarly, on expressing the moments (M_{ye},M_{yele},M_{ym}) in terms of transverse deflection (w) from Eq.(17) one obtains,

$$\left\{D\nabla^4w+E\nabla^4w+M\nabla^4w\right\}=-\rho h\frac{\partial^2w}{\partial t^2}+\frac{\partial^2M_{Tx}}{\partial x^2}+\frac{\partial^2M_{Ty}}{\partial y^2}-N_{Tx}\frac{\partial^2w}{\partial x^2}-N_{Ty}\frac{\partial^2w}{\partial y^2}$$
$$+\frac{2a}{3\left(\frac{\delta_{bt}}{6}+\delta_{bb}\right)\left(3+\nu\right)\left(1-\nu\right)h+2a}\left[\frac{h^3}{12}\left\{\tilde{c}_{12}\frac{\partial^4w}{\partial x^2y^2}+\tilde{c}_{11}\frac{\partial^4w}{\partial y^4}+\tilde{e}_{31}\frac{\Delta_1}{\Delta}\left(\frac{\partial^4w}{\partial x^2y^2}+\frac{\partial^4w}{\partial y^4}\right)+q_{31}\frac{\Delta_2}{\Delta}\left(\frac{\partial^4w}{\partial x^2y^2}+\frac{\partial^4w}{\partial y^4}\right)\right\}-\frac{\partial^2M_{Ty}}{\partial y^2}\right]- \tag{30}$$
$$\frac{2a}{\left(6\delta_{bt}+\delta_{tt}\right)\left(1-\nu^2\right)h+2a}N_{Ty}\frac{\partial^2w}{\partial y^2}+P_z$$

3 RELATION FOR NATURAL FREQUANCY

The presence of external environment like rise in temperature has been included in the governing equation of cracked plate in the form of thermal bending moments and in-plane compressive forces. Three significant solution cases arise by the presence of thermal environment; (1) the plate is heated throughout its volume uniformly $(M_{Tx}=M_{Ty}=0)$ with in-plane deflections restricted (2) Unrestricted in-plane deflections ($N_{Tx}=N_{Ty}=0$) and only thermal moment (3) The third solution can be found for presence of both thermal bending and in-plane compressive thermal forces. The present work restricts itself to the formulation of governing equation for all the above three cases and give results for case (1). Since, in majority of engineering applications thin plate structures

having good thermal conductivity are used, there is little temperature gradient along the thickness of the plate and they can be considered as uniformly heated plates. The constant in-plane compressive forces induced due to temperature are only considered making the model geometrically linear. So, for a plate in the absence of thermal moments ($M_{Tx} = M_{Ty} = 0$) and the presence of constant in-plane compressive forces (N_{Tx} and N_{Ty}) due to uniform rise in temperature, the governing equation (Eq. (30)) becomes

$$\left\{D\nabla^4 w + E\nabla^4 w + M\nabla^4 w\right\} = -\rho h\frac{\partial^2 w}{\partial t^2} - N_{Tx}\frac{\partial^2 w}{\partial x^2} - N_{Ty}\frac{\partial^2 w}{\partial y^2} + \frac{2a}{3\left(\frac{\delta_{bt}}{6}+\delta_{bb}\right)(3+\nu)(1-\nu)h+2a}$$
$$\left[\frac{h^3}{12}\left\{\tilde{c}_{12}\frac{\partial^4 w}{\partial x^2 y^2} + \tilde{c}_{11}\frac{\partial^4 w}{\partial y^4} + \tilde{e}_{31}\frac{\Delta_1}{\Delta}\left(\frac{\partial^4 w}{\partial x^2 y^2} + \frac{\partial^4 w}{\partial y^4}\right) + q_{31}\frac{\Delta_2}{\Delta}\left(\frac{\partial^4 w}{\partial x^2 y^2} + \frac{\partial^4 w}{\partial y^4}\right)\right\}\right] - \frac{2a}{\left(6\delta_{bt}+\delta_{tt}\right)\left(1-\nu^2\right)h+2a}N_{Ty}\frac{\partial^2 w}{\partial y^2} + P_z \tag{31}$$

On substituting the Eq.(13) and (14) into Eq.(1), integrating them with respect to *z*-direction over the plate thickness and neglecting the in-plane forces due to lateral deflection of plate. The required expression for in-plane forces due to thermal environment only can be proposed as:

$$N_{Tx} = N_{Ty} = \left(\beta_1 - \tilde{e}_{31}\frac{\Delta_3}{\Delta} - q_{31}\frac{\Delta_4}{\Delta}\right)\int_{-\frac{h}{2}}^{+\frac{h}{2}} T(z)\,dz \tag{32}$$

For a uniform heated plate, the constant in-plane forces given in Eq. (32) can be reduced as:

$$N_{Tx} = N_{Ty} = \left(\beta_1 - \tilde{e}_{31}\frac{\Delta_3}{\Delta} - q_{31}\frac{\Delta_4}{\Delta}\right)hT_c \tag{33}$$

where T_c is the temperature rise above the temperature at which the plate is stress free. On substituting Eq. (33) into Eq. (31) one obtains

$$\left\{D\nabla^4 w + E\nabla^4 w + M\nabla^4 w\right\} = -\rho h\frac{\partial^2 w}{\partial t^2} - \left(\beta_1 - \tilde{e}_{31}\frac{\Delta_3}{\Delta} - q_{31}\frac{\Delta_4}{\Delta}\right)hT_c\left(\frac{\partial^2 w}{\partial x^2} + \frac{\partial^2 w}{\partial y^2}\right) + \frac{2a}{3\left(\frac{\delta_{bt}}{6}+\delta_{bb}\right)(3+\nu)(1-\nu)h+2a}$$
$$\left[\frac{h^3}{12}\left\{\tilde{c}_{12}\frac{\partial^4 w}{\partial x^2 y^2} + \tilde{c}_{11}\frac{\partial^4 w}{\partial y^4} + \tilde{e}_{31}\frac{\Delta_1}{\Delta}\left(\frac{\partial^4 w}{\partial x^2 y^2} + \frac{\partial^4 w}{\partial y^4}\right) + q_{31}\frac{\Delta_2}{\Delta}\left(\frac{\partial^4 w}{\partial x^2 y^2} + \frac{\partial^4 w}{\partial y^4}\right)\right\}\right] - \frac{2a}{\left(6\delta_{bt}+\delta_{tt}\right)\left(1-\nu^2\right)h+2a}\left(\widetilde{\beta_1 - e_{31}}\frac{\Delta_3}{\Delta} - \widetilde{q_{31}}\frac{\Delta_4}{\Delta}\right)hT_c\frac{\partial^2 w}{\partial y^2} + P_z \tag{34}$$

Assuming the solution for lateral deflection as:

$$w(x, y, t) = W_{mn}\sin\left(\frac{m\pi x}{l_1}\right)\sin\left(\frac{n\pi y}{l_2}\right)\sin(\omega t) \tag{35}$$

where, ω is the vibrational frequency. On substituting the expression of lateral deflection from Eq. (35) into Eq. (34), one can obtain the natural frequencies (ω_{mn}) of cracked MEE plate in presence of thermal environment as:

$$\omega_{mn} = \sqrt{\frac{\pi^4(D+E+M)\left(\left(\frac{m}{l_1}\right)^2 + \left(\frac{n}{l_2}\right)^2\right)^2 - \frac{2a}{H_2}\frac{\pi^4 h^3}{12}\left\{\tilde{c}_{11}\left(\frac{n}{l_2}\right)^4 + \tilde{c}_{12}\frac{m^2 n^2}{l_1^2 l_2^2} + \left(\tilde{e}_{31}\frac{\Delta_1}{\Delta} + q_{31}\frac{\Delta_2}{\Delta}\right)\left(\frac{m^2 n^2}{l_1^2 l_2^2} + \left(\frac{n}{l_2}\right)^4\right)\right\} - hT_c\pi^2\left(\beta_1 - \tilde{e}_{31}\frac{\Delta_3}{\Delta} - q_{31}\frac{\Delta_4}{\Delta}\right)\left(\left(\frac{m}{l_1}\right)^2 + \left(\frac{n}{l_2}\right)^2 + \frac{2a}{H_1}\left(\frac{n}{l_2}\right)^2\right)}{\rho h}} \tag{36}$$

where, $H_2 = 3\left(\frac{\delta_{bt}}{6} + \delta_{bb}\right)(3+\nu)(1-\nu)h + 2a$ and $H_1 = \left(6\delta_{bt} + \delta_{tt}\right)\left(1-\nu^2\right)h + 2a.$ For a special case of a square plate with side of l_1 and $m = n = 1$, the natural frequency ω_{11} takes the form which clearly shows the presence of crack and temperature terms.

$$\omega_{11} = \sqrt{\frac{\frac{\pi^4}{l_1^4}\left[4\left(D+E+M\right) - \frac{2a}{H_2}\frac{h^3}{12}\left\{\tilde{c}_{11} + \tilde{c}_{12} + 4\left(\tilde{e}_{31}\frac{\Delta_1}{\Delta} + q_{31}\frac{\Delta_2}{\Delta}\right)\right\} - \frac{l_1^2 h T_c}{\pi^2}(2+\frac{2a}{H_1})\left(\beta_1 - \tilde{e}_{31}\frac{\Delta_3}{\Delta} - q_{31}\frac{\Delta_4}{\Delta}\right)\right]}{\rho h}} \tag{37}$$

On neglecting the crack ($a = 0$) and the temperature ($T_c = 0$) terms from Eq. (37), one can find the natural frequencies of intact MEE plate as:

$$\omega_{11}^{intact} = \sqrt{\frac{\frac{\pi^4}{l_1^4}\left[4\left(D+E+M\right)\right]}{\rho h}} \tag{38}$$

4 RELATION FOR CRITICAL BUCKLING TEMOERATURE

Like the mechanical buckling, thermal buckling implies the out of plane deformation due to in-plane compressive forces produced by the rise in temperature. Thermal buckling is an equilibrium position between stiffness and in-plane temperature forces satisfying the boundary conditions. When a restrained plate is uniformly heated then due to developed thermal stresses, it buckles at a specific temperature [49]. Literature Ref. [49] and [41] shows the classical relation for buckling temperature for an intact and cracked isotropic plate respectively. A unique classical relation for buckling temperature for cracked MEE plate is derived in this section. The material properties are assumed to be independent of temperature. For geometrically linear i.e. $M_{Tx} = M_{Ty} = 0$ and constant in-plane forces due to uniform rise in temperature N_{Tx} and N_{Ty}; only the static and no kinematic boundary conditions have to be satisfied (Ref. [50]).

Consider the cracked MEE plate element with all edges simply supported with in-plane displacement restricted, shown in Fig. 2. It is known that at buckling temperature, the fundamental frequency for an intact plate becomes zero (Ref. [51]) there by making the stiffness of the plate as zero. This is equally true for the cracked plate also. So, in the absence of thermal bending and the presence of constant in-plane forces due to uniform rise in temperature; the equation of equilibrium (Eq. (39)) for cracked MEE plate can be obtained by equating the stiffness to zero.

$$\begin{aligned}&\left\{D\nabla^4 w + E\nabla^4 w + M\nabla^4 w\right\} - \frac{2a}{H_2}\left[\frac{h^3}{12}\left\{\tilde{c}_{12}\frac{\partial^4 w}{\partial x^2 y^2} + \tilde{c}_{11}\frac{\partial^4 w}{\partial y^4} + \tilde{e}_{31}\frac{\Delta_1}{\Delta}\left(\frac{\partial^4 w}{\partial x^2 y^2} + \frac{\partial^4 w}{\partial y^4}\right) + q_{31}\frac{\Delta_2}{\Delta}\left(\frac{\partial^4 w}{\partial x^2 y^2} + \frac{\partial^4 w}{\partial y^4}\right)\right\}\right] = \\ &-\left(\beta_1 - \tilde{e}_{31}\frac{\Delta_3}{\Delta} - q_{31}\frac{\Delta_4}{\Delta}\right)hT_c\left(\frac{\partial^2 w}{\partial x^2} + \frac{\partial^2 w}{\partial y^2} + \frac{2a}{H_1}\frac{\partial^2 w}{\partial y^2}\right)\end{aligned} \tag{39}$$

Assuming the solution as:

$$w(x,y) = W'_{mn}\sin\left(\alpha_m x\right)\sin\left(\beta_n y\right) \tag{40}$$

where $\alpha_m = \frac{m\pi}{l_1}$ and $\beta_n = \frac{n\pi}{l_2}$. Using Eq. (39) the expression for buckling temperature of a cracked MEE plate can be simplified as:

$$T_{bcr}=\frac{h^2\pi^2\left[\left(\tilde{c}_{11}+\tilde{e}_{31}\frac{\Delta_1}{\Delta}+q_{31}\frac{\Delta_2}{\Delta}\right)\left(m^2\left(\frac{l_2}{l_1}\right)^2+n^2\right)^2-\frac{2a}{H_2}\left\{\tilde{c}_{11}n^4+\tilde{c}_{12}m^2n^2\left(\frac{l_2}{l_1}\right)^2+\left(\tilde{e}_{31}\frac{\Delta_1}{\Delta}+q_{31}\frac{\Delta_2}{\Delta}\right)\left(n^4+m^2n^2\left(\frac{l_2}{l_1}\right)^2\right)\right\}\right]}{12l_2^2\left(\beta_1-\tilde{e}_{31}\frac{\Delta_3}{\Delta}-q_{31}\frac{\Delta_4}{\Delta}\right)\left(m^2\left(\frac{l_2}{l_1}\right)^2+n^2\left(1+\frac{2a}{H_1}\right)\right)} \tag{41}$$

From Eq. (41), the critical buckling temperature T_{bcr} can be evaluated for $m=n=1$, as for other values of *m* and *n*, the buckling temperature obtained is higher. For an un-cracked (intact) MEE plate ($2a = 0$) Eq. (41) can be written as:

$$T_{bcr}=\frac{h^2\pi^2\left[\left(\tilde{c}_{11}+\tilde{e}_{31}\frac{\Delta_1}{\Delta}+q_{31}\frac{\Delta_2}{\Delta}\right)\left(m^2\left(\frac{l_2}{l_1}\right)^2+n^2\right)^2\right]}{12l_2^2\left(\beta_1-\tilde{e}_{31}\frac{\Delta_3}{\Delta}-q_{31}\frac{\Delta_4}{\Delta}\right)\left(m^2\left(\frac{l_2}{l_1}\right)^2+n^2\right)} \tag{42}$$

It is important here to mention that the literature lacks in classical thermal buckling relation for MEE intact and cracked plate. The present work proposes such relations given by Eq.(41) and Eq.(42) respectively. These relations clearly show the effect of electric, magnetic and thermal fields on critical buckling temperature.

5 RELATION FOR CENTRAL DEFLECTION OF PLATE

Consider a transversely isotropic magneto-electro-thermo-elastic cracked plate with all edges simply supported, subjected to a lateral uniformly distributed dynamic load (P_z) harmonically varying with time. For a plate in the absence of thermal bending ($M_{Tx}=M_{Ty}=0$) and the presence of constant in-plane forces (N_{Tx} and N_{Ty}) due to uniform rise in temperature, the governing equation (Eq. (30)) becomes

$$\begin{aligned}&\{D+E+M\}\nabla^4 w-\frac{2a}{H_2}\left[\frac{h^3}{12}\left\{\tilde{c}_{12}\frac{\partial^4 w}{\partial x^2 y^2}+\tilde{c}_{11}\frac{\partial^4 w}{\partial y^4}+\tilde{e}_{31}\frac{\Delta_1}{\Delta}\left(\frac{\partial^4 w}{\partial x^2 y^2}+\frac{\partial^4 w}{\partial y^4}\right)+q_{31}\frac{\Delta_2}{\Delta}\left(\frac{\partial^4 w}{\partial x^2 y^2}+\frac{\partial^4 w}{\partial y^4}\right)\right\}\right]+\\&\left(\beta_1-\tilde{e}_{31}\frac{\Delta_3}{\Delta}-q_{31}\frac{\Delta_4}{\Delta}\right)hT_c\left(\frac{\partial^2 w}{\partial x^2}+\frac{\partial^2 w}{\partial y^2}+\frac{2a}{H_1}\frac{\partial^2 w}{\partial y^2}\right)+\rho h\frac{\partial^2 w}{\partial t^2}=\mathrm{P}_z\end{aligned} \tag{43}$$

Assuming the solution for lateral deflection as:

$$w(x,y,t)=W_{mn}\sin\left(\frac{m\pi x}{l_1}\right)\sin\left(\frac{n\pi y}{l_2}\right)\sin(\omega t) \tag{44}$$

where, ω is the vibrational frequency. Now for the case of forced flexural vibrations, the applied dynamic lateral load $P_z=P_z(x,y,t)$ can be expressed as: [68]

$$P_z(x,y,t)=P_{mn}\sin\left(\frac{m\pi x}{l_1}\right)\sin\left(\frac{n\pi y}{l_2}\right)\sin(\varnothing t) \tag{45}$$

with $\varnothing$ being the operational frequency of the load. Substituting the general solution of lateral deflection (w) from Eq. (44) with ω being replaced by $\varnothing$ and the lateral dynamic load (P_z) form Eq. (45) into the governing equation

(Eq. (43)) results in an expression for W_{mn} . Thus the classical relation for central deflection of cracked MEE plate in the presence of thermal environment can be proposed as:

$$W_{mn}=\frac{P_{mn}}{\pi^4\left(D+E+M\right)\left(\left(\frac{m}{l_1}\right)^2+\left(\frac{n}{l_2}\right)^2\right)^2-\frac{2a}{H_2}\frac{\pi^4h^3}{12}\left\{\tilde{c}_{11}\left(\frac{n}{l_2}\right)^4+\tilde{c}_{12}\frac{m^2n^2}{l_1^2l_2^2}+\left(\tilde{e}_{31}\frac{\Delta_1}{\Delta}+q_{31}\frac{\Delta_2}{\Delta}\right)\left(\frac{m^2n^2}{l_1^2l_2^2}+\left(\frac{n}{l_2}\right)^4\right)\right\}} \\ -hT_c\pi^2\left(\beta_1-\tilde{e}_{31}\frac{\Delta_3}{\Delta}-q_{31}\frac{\Delta_4}{\Delta}\right)\left(\left(\frac{m}{l_1}\right)^2+\left(\frac{n}{l_2}\right)^2+\frac{2a}{H_1}\left(\frac{n}{l_2}\right)^2\right)-\varnothing^2\rho h \tag{46}$$

For a special case of a square plate with side of l_1 and $m=n=1$, the central deflection W_{11} takes the form which clearly shows the presence of crack term and temperature terms.

$$W_{11}=\frac{P_{11}}{\frac{\pi^4}{l_1^4}\left[4\left(D+E+M\right)-\frac{2a}{H_2}\frac{h^3}{12}\left\{\tilde{c}_{11}+\tilde{c}_{12}+4\left(\tilde{e}_{31}\frac{\Delta_1}{\Delta}+q_{31}\frac{\Delta_2}{\Delta}\right)\right\}-\frac{l_1^2hT_c}{\pi^2}\left(2+\frac{2a}{H_1}\right)\left(\beta_1-\tilde{e}_{31}\frac{\Delta_3}{\Delta}-q_{31}\frac{\Delta_4}{\Delta}\right)\right]-\varnothing^2\rho h} \tag{47}$$

The result for central deflection of a cracked MEE plate without influence of thermal environment can be expressed as:

$$W_{11}^{\ cracked}=\frac{P_{11}}{\frac{\pi^4}{l_1^4}\left[4\left(D+E+M\right)-\frac{2a}{H_2}\frac{h^3}{12}\left\{\tilde{c}_{11}+\tilde{c}_{12}+4\left(\tilde{e}_{31}\frac{\Delta_1}{\Delta}+q_{31}\frac{\Delta_2}{\Delta}\right)\right\}\right]-\varnothing^2\rho h} \tag{48}$$

Similarly, the central deflection of a uniformly heated MEE plate without any crack can be expressed as:

$$W_{11}^{\ heated}=\frac{P_{11}}{\frac{\pi^4}{l_1^4}\left[4\left(D+E+M\right)-\frac{2l_1^2hT_c}{\pi^2}\left(\beta_1-\tilde{e}_{31}\frac{\Delta_3}{\Delta}-q_{31}\frac{\Delta_4}{\Delta}\right)\right]-\varnothing^2\rho h} \tag{49}$$

The central deflection of an intact MEE plate ($a=0,\ T_c=0$)

$$W_{11}^{\ intact}=\frac{P_{11}}{\frac{\pi^4}{l_1^4}\left[4\left(D+E+M\right)\right]-\varnothing^2\rho h} \tag{50}$$

The central deflection ratio $W_{11}^{\ cracked}/W_{11}^{\ intact}$ can be obtained by dividing Eq. (48) and Eq. (50) as:

$$\frac{W_{11}^{\ cracked}}{W_{11}^{\ intact}}=\frac{\frac{\pi^4}{l_1^4}\left[4\left(D+E+M\right)\right]-\varnothing^2\rho h}{\frac{\pi^4}{l_1^4}\left[4\left(D+E+M\right)-\frac{2a}{H_2}\frac{h^3}{12}\left\{\tilde{c}_{11}+\tilde{c}_{12}+4\left(\tilde{e}_{31}\frac{\Delta_1}{\Delta}+q_{31}\frac{\Delta_2}{\Delta}\right)\right\}\right]-\varnothing^2\rho h} \tag{51}$$

or

$$\frac{W_{11}^{\ cracked}}{W_{11}^{\ intact}}=\frac{1-\left(\varnothing/\omega_{11}^{intact}\right)^2}{1-\frac{\frac{2a}{H_2}\frac{h^3}{12}\left\{\tilde{c}_{11}+\tilde{c}_{12}+4\left(\tilde{e}_{31}\frac{\Delta_1}{\Delta}+q_{31}\frac{\Delta_2}{\Delta}\right)\right\}}{4\left(D+E+M\right)}-\left(\varnothing/\omega_{11}^{intact}\right)^2} \tag{52}$$

where, $\omega_{11}^{intact} = \sqrt{\dfrac{\pi^4}{l_1^4}\left[4\left(D+E+M\right)\right]}{\rho h}$ is the natural frequency of intact MEE plate. Similarly, the central deflection ratio $W_{11}^{heated}/W_{11}^{intact}$ can be obtained by dividing Eq. (49) and Eq. (50) as:

$$\frac{W_{11}^{heated}}{W_{11}^{intact}} = \frac{1-\left(\varnothing/\omega_{11}^{intact}\right)^2}{1-\dfrac{2l_1^2hT_c}{\pi^2}\left(\beta_1-\tilde{e}_{31}\dfrac{\Delta_3}{\Delta}-q_{31}\dfrac{\Delta_4}{\Delta}\right)\Big/4\left(D+E+M\right)-\left(\varnothing/\omega_{11}^{intact}\right)^2} \tag{53}$$

6 RESULTS AND DISCUSSION

In this section, the analytical results for free vibration and buckling of partially cracked MEE plate in presence of thermal environment are presented. Since the literature lacks in results for cracked MEE plate under influence of the thermal environment, new results for frequencies of plate are presented as a function half crack length (a), plate aspect ratio $\left(\dfrac{l_1}{l_2}\right)$ and uniform rise in non-dimensional temperature $(T^* = T_{(c)}/T_{(bcr)})$. The MEE plate specimen considered is made up of a fiber reinforced $BaTiO_3$–$CoFe_2O_4$ composite for the analysis with material properties listed in Table 1. The volume fraction of $BaTiO_3$ and $CoFe_2O_4$ for this MEE composite is assumed to be fixed at 50% for the analysis.

Table 1
Material constant for thin MEE $BaTiO_3$ - $CoFe_2O_4$ composite plates. [3], [30]

Properties	$BaTiO_3$–$CoFe_2O_4$
Elastic (10^9 N/m^2)	c_{11} = 226, c_{12} = 125, c_{13} = 124, c_{33} = 216, c_{44} = 44, c_{66} = 50
Piezoelectric (C/m^2)	e_{31} = -2.2, e_{33} = 9.3, e_{15} = 5.8
Piezomagnetic (N/Am^2)	q_{31} = 290.1, q_{33} = 349.9, q_{15} = 275
Dielectric (10^{-9} $C^2/N\,m^2$)	E_{11} = 5.64, E_{33} = 6.35
Magnetic (10^{-6} $N\,s^2/C^2$)	μ_{11} = -2.97, μ_{33} = 83.5
Magnetoelectric (10^{-12} $N\,s/VC$)	d_{11} = 5.367, d_{33} = 2737.5
Thermal moduli (10^5 $NK^{-1}m^{-2}$)	β_1 = 4.74, β_3 = 4.53
Pyroelectric (10^{-6} CN^{-1})	P_3 = 25
Pyromagnetic (10^{-6} $NA^{-1}m^{-1}K^{-1}$)	τ_3 = 5.19
Mass density (kgm^{-3})	ρ = 5550

For aiming to validate the present model the analytical solution obtained using present study is first applied to the case of pure thin elastic plate in absence of thermal environment. For a purely thin elastic plate, it is known that the piezomagnetic and piezoelectric effects will vanish i.e., $M = 0$ and $E = 0$. The non-dimensional frequency parameter $\left(\omega_{mn}L_1^2\sqrt{\rho h/D}\right)$ for a thin elastic plate having in-plane dimensions $l_1 = l_2 = 1m$ and thickness $h = 0.01m$ are recorded along with the existing results from literature (Ref. [23] [41] [52]) in Table 2. It is seen that the listed results show good agreement which verifies the validity of the present model.

Table 2
Non dimensional frequency parameter $\left(\omega_{mn}L_1^2\sqrt{\rho h/D}\right)$ for intact thin elastic plate. (E = M = 0, T = 0)

Boundary condition	Present	Ref. [52]	Ref. [41]	Ref. [23]
SSSS	19.739	19.739	-	19.739
CCSS	28.348	28.350	28.350	-

Since most of the research work on analysis of intact magneto-electro-elastic (MEE) plates has been performed using the higher order theories, the obtained results of present study are compared with those offered by the higher order theories in order to show the efficacy of the present model. Such comparison of results for frequency parameter $\left(\omega_{mn} l_1 \sqrt{\rho / c_{max}}\right)$ of intact MEE plate obtained using the present theory (CPT) and the higher order theory (HSDT) is shown in Table 3. The material properties for the plate are taken from Ref. [23] for comparing the results of Table 3. The obtained results from the present theory are slightly higher than the existing results of Ref. [23] because of ignoring the rotary inertia and effect of shear deformation in the present model. Regardless of the overestimate on the results caused by imposing the plate theory to MEE plate, the present model has obvious advantage of being fast, efficient, ease of parametric study and conservative prediction for the vibration characteristics.

Table 3

Non dimensional frequency parameter $\left(\omega_{mn} l_1 \sqrt{\rho / c_{max}}\right)$ for intact MEE plate. (h= 1mm, $l_1 / h = 10$)

Boundary condition	Aspect ratio (L_1 / L_2)	Present (CPT)	Ref. [23] (HSDT)
SSSS	0.5	0.366	0.343
	1	0.585	0.535
	2	1.463	1.233
CCCC	0.5	0.730	0.675
	1	1.070	0.962
	2	2.923	2.342

The literature on vibration analysis of plate lacks in the results for cracked MEE plate due to coupling of electro-elasto-magnetic effects. These effects are further complicated in the presence of thermal environment which induces pyroeffects. Thus no work has been done on vibration analysis of cracked magneto-electro-thermo-elastic plates and hence the validation of present model is carried out for cracked isotropic plate under influence of thermal environment. Table 4., shows the validation of results for dimensionless frequency parameter of cracked isotropic plate under CCSS boundary condition. The plate dimensions and mechanical properties are: $l_1 = l_2 = 1m$, thickness $h = 0.01m$, Young's modulus $E = 70.3GPa$, material density $\rho = 2660kg / m^{-3}$ and Poisson's ratio $v = 0.33$. From Table 4., it can be concluded that the results for intact and cracked isotropic plate can be computed with good precision when compared to the results of Ref. [41].

Table 4

Non dimensional frequency parameter $\left(\omega_{mn} L_1^2 \sqrt{\rho h / D}\right)$ of intact and cracked isotropic plate for CCSS boundary condition. ($E = M = 0$)

Half Crack Length (a / l_1)	$T^*\left(T_c / T_{bcr}\right)$					
	$T^* = 0.1$		$T^* = 0.2$		$T^* = 0.3$	
	Present	Ref [41]	Present	Ref [41]	Present	Ref [41]
0	26.89	26.89	25.35	25.35	23.72	23.72
0.01	25.95	26.00	24.45	24.51	22.85	22.93
0.05	23.91	24.17	22.49	22.78	20.96	21.31

The results for natural frequencies of the cracked magneto-electro-thermo-elastic plate as affected by length of crack (a), uniform rise in temperature (T^*) and mode number (m, n) are given next. To study the effect of thermal environment on cracked MEE plate, the results for natural frequency are listed in Table 5., for simply supported boundary condition. The material constants of the plate are taken from Table 1. The plate dimensions are assumed as $l_1 = l_2 = 1m$ and $h = 0.01m$. The effective Poisson's (v) ratio of MEE plate specimen is assumed to be constant at 0.3 in the present work. The crack depth to plate thickness ratio is taken as 0.6 and the length of the crack 2a is located at the centre of plate. The uniform rise in temperature is represented as non-dimensional temperature $T^*\left(T_c / T_{bcr}\right)$ where T_c and T_{bcr} are the rise in temperature and critical buckling temperature respectively.

The influence of temperature variation on natural frequencies of cracked isotropic plate is well established in literature; Table 5., shows such results for cracked magneto-electro-thermo-elastic plate for a given crack length and mode number. It is seen that for all the different modes of vibration, for a given crack length, as the plate's temperature (T^*) is increased, the frequencies go on decreasing as result of decrease in stiffness of plate due to the thermal stresses. Similarly, for a given rise in temperature (T^*) of plate when the length of crack increases, the natural frequencies decrease as a result of reduction in stiffness of MEE plate. Such lower values of frequencies are evident for cracked isotropic plates in absence of thermal effects from the works of Refs. [35–37]. It is interesting to see that with increase in crack length (a), the natural frequency decreases significantly for 2^{nd} mode of vibration. It is because in the 2^{nd} mode of vibration when plate vibrates symmetric with respect to x axis, one nodal line overlaps and no nodal line intersects the crack which decreases frequency more with increase in crack length (a). Such lower values of frequencies for second mode are also evident for cracked plates in vacuum from the works of Refs. [53]. Thus it is concluded that effect of crack on second mode is more pronounced than the other three modes of vibration.

Table 5
Fundamental frequencies ω_{mn} (*Rad/sec*) for SSSS MEE plate.

T^*	Half crack length a (m)	Mode (m, n)			
		(1, 1)	(1, 2)	(2, 1)	(2, 2)
0	0	310.56	776.41	776.41	1242.26
	0.05	284.27	635.45	757.86	1137.07
	0.1	274.21	576.48	751.09	1096.84
	0.15	268.89	543.64	747.58	1075.55
0.1	0	294.63	736.57	736.57	1178.51
	0.05	269.68	602.84	718.97	1078.72
	0.1	260.14	546.90	712.55	1040.55
	0.15	255.09	515.75	709.22	1020.35
0.2	0	277.78	694.44	694.44	1111.11
	0.05	254.26	568.36	677.85	1017.03
	0.1	245.26	515.62	671.80	981.04
	0.15	240.50	486.25	668.66	962.00
0.3	0	259.84	649.59	649.59	1039.35
	0.05	237.84	531.65	634.07	951.34
	0.1	229.42	482.32	628.41	917.68
	0.15	224.97	454.85	625.47	899.87
0.4	0	240.56	601.41	601.41	962.25
	0.05	220.19	492.22	587.04	880.77
	0.1	212.40	446.54	581.79	849.61
	0.15	208.28	421.11	579.08	833.11
0.5	0	219.60	549.01	549.01	878.41
	0.05	201.01	449.33	535.89	804.03
	0.1	193.90	407.63	531.10	775.58
	0.15	190.13	384.41	528.62	760.53
0.6	0	196.42	491.05	491.05	785.67
	0.05	179.79	401.89	479.32	719.15
	0.1	173.43	364.60	475.03	693.70
	0.15	170.06	343.83	472.81	680.24
0.7	0	170.10	425.26	425.26	680.41
	0.05	155.70	348.05	415.10	622.80
	0.1	150.19	315.75	411.39	600.76
	0.15	147.28	297.77	409.47	589.10
0.8	0	138.89	347.22	347.22	555.56
	0.05	127.13	284.18	338.93	508.51
	0.1	122.63	257.81	335.90	490.52
	0.15	120.25	243.13	334.33	481.00
0.9	0	98.21	245.52	245.52	392.84
	0.05	89.89	200.95	239.66	359.57
	0.1	86.71	182.30	237.52	346.85
	0.15	85.03	171.92	236.41	340.12

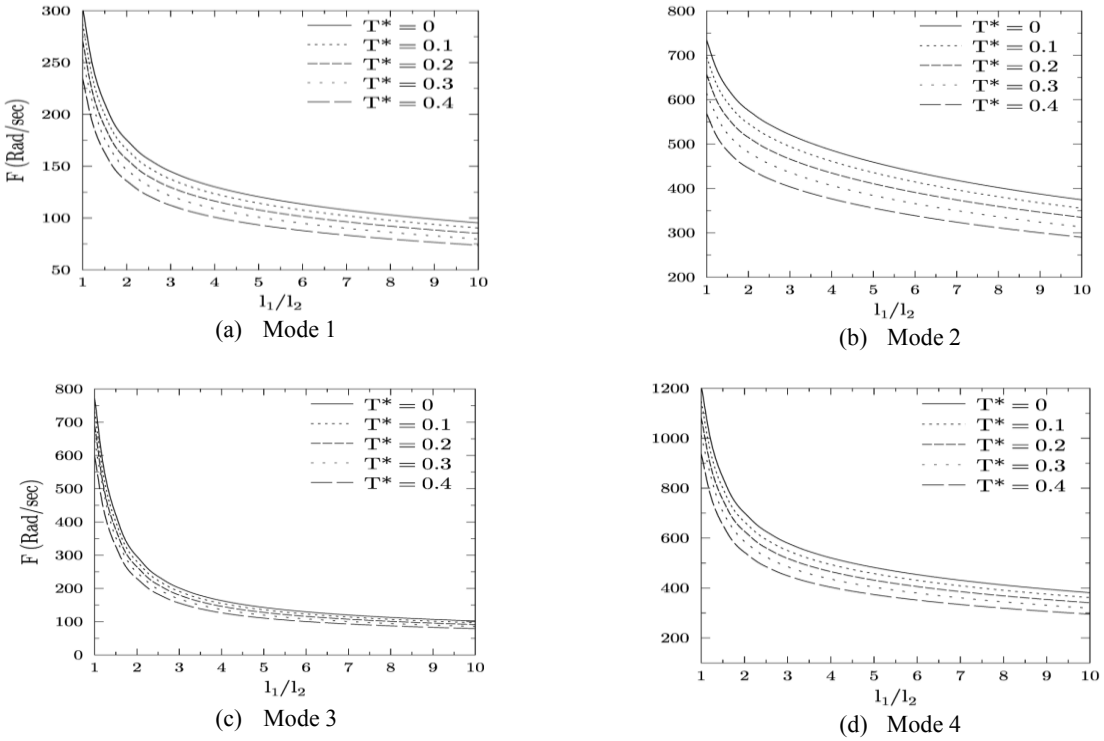

(a) Mode 1 (b) Mode 2

(c) Mode 3 (d) Mode 4

Fig.5
Variation of fundamental frequencies with T^* for various plate aspect ratio, $a/l_1 = 0.01$.

The variations in fundamental frequencies with rise in temperature (T^*) and plate aspect ratio (l_1/l_2), for fixed crack length ($a/l_1 = 0.01$) is shown in Fig. 5. It is seen that for all values of plate aspect ratio, the uniform rise in temperature decreases the fundamental frequencies of the cracked plate which satisfies one's intuition. Thus the presence of thermal environment decreases the fundamental frequencies of the plate. Also comparing the decrease in Fig. 5(a) to (d), it is seen that effect of the rise in temperature is more pronounced for the second mode of vibration as compare to other modes. Similarly, for all values of T^*, the fundamental frequency decreases with increase in plate aspect ratio.

Fig. 6 shows the variation of fundamental frequency with plate aspect ratio (l_1/l_2) and crack length (a/l_1), for fixed temperature ($T^* = 0.1$). Comparing the variation in Fig. 6(a) to (d), it is observed that for all plate aspect ratio the fundamental frequency decreases with increase in length of crack and this decrease in more significant for second mode of vibration. Similarly, for a given crack length, the fundamental frequency decreases with increase in plate aspect ratio. Also comparing the difference in fundamental frequencies in Fig. 6(a) to (d), it is seen that this difference increases with the increase in length of crack and plate aspect ratio.

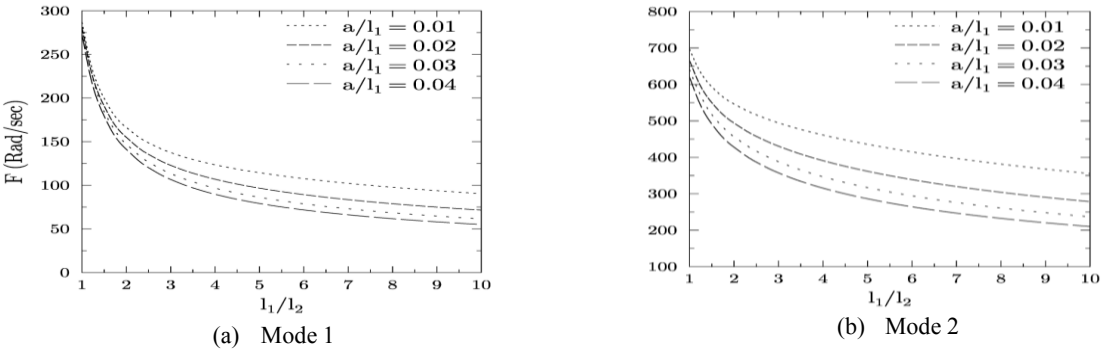

(a) Mode 1 (b) Mode 2

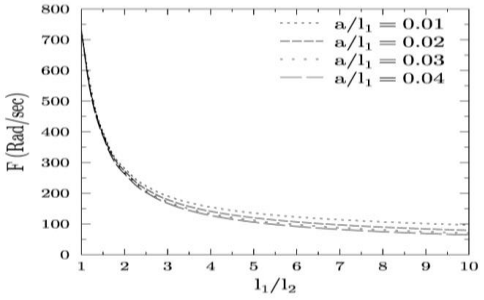

(c) Mode 3

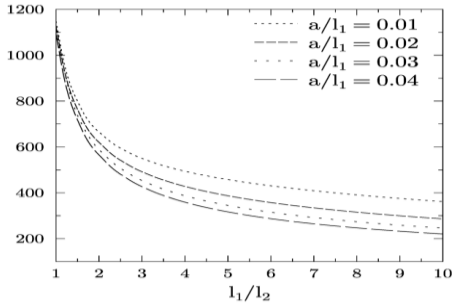

(d) Mode 4

Fig.6
Variation of fundamental frequencies with l_1 / l_2 for various crack length, $T^* = 0.1$.

The variation in dimensionless critical buckling temperature $\left(T_{bcr-cra.} / T_{bcr-intact}\right)$ of cracked MEE plate with plate aspect ratio $\left(l_1 / l_2\right)$ and crack length ratio, for four different modes of vibration is shown in Fig. 7(a) to (d). It is seen that for all values of plate aspect ratio, the increase in length of crack from $a / l_1 = 0.05$ to 0.2, decreases the buckling temperature. Thus it is concluded that the presence of crack diminishes the buckling temperature of MEE plate which satisfies one's physical understanding. Similarly, with increase in plate aspect ratio the critical buckling temperature decreases for given crack length ratio. Fig. 8 shows the variation of critical buckling temperature with thickness for first mode of vibration. It is observed that for a given plate thickness the buckling temperature decreases in the presence of crack. Further as the plate becomes thin with increase in l_1 / h, the buckling temperature decreases which is true from one's physical understanding.

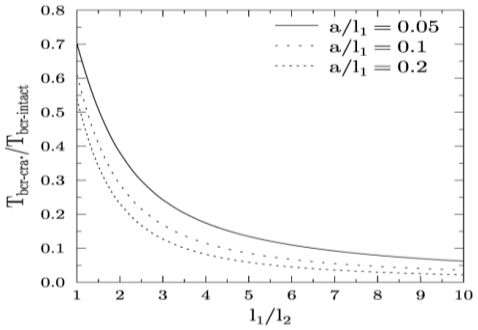

(a) Mode 1

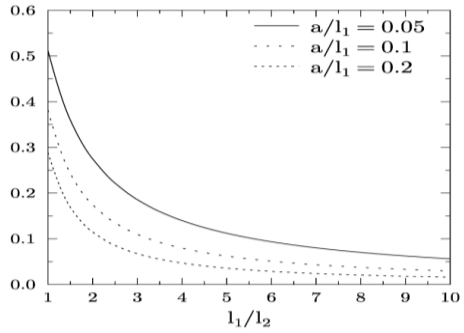

(b) Mode 2

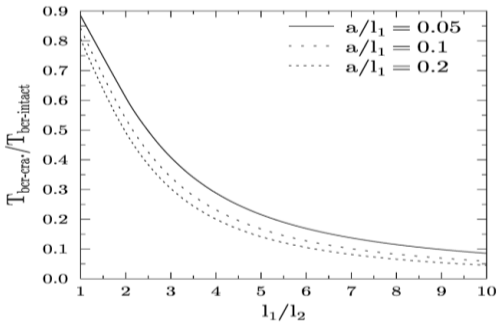

(c) Mode 3

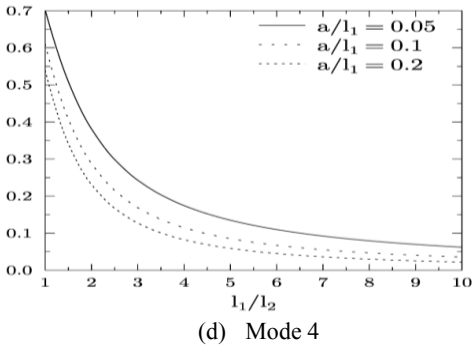

(d) Mode 4

Fig.7
Variation of non-dimensional critical buckling temperature with l_1 / l_2 for various crack lengths.

Fig. 9 shows the variation of ratio of deflection of cracked plate to intact MEE plate. In order to investigate the primary resonance, the ratio of forcing frequency to fundamental frequency of intact plate is varied from 0.5 to 1.4.

It is interesting to note that the presence of crack shifts the primary resonance and it takes place well below $\varnothing / \omega_{11}^{intact} = 1$. This is due to decrease in stiffness of plate due to centrally located crack. The results for variation of deflection ratio of heated intact plate to intact plate with respect to ratio of forcing frequency and fundamental frequency are shown in Fig. 10. With the rise in temperature of plate, it is known that the fundamental frequencies decreases, such a fact seen in literature is validated from the results in Fig. 10. As expected the rise of temperature decreases fundamental frequency of plate thereby increasing the deflection. The shift in primary resonance can be attributed to the decrease in stiffness due to temperature rise. Thus to the best of authors knowledge Figs. 9 and 10 along with Eqs.(46) to (53) presents first time the effect of rise in temperature, crack length on deflection and primary resonance of MEE plate.

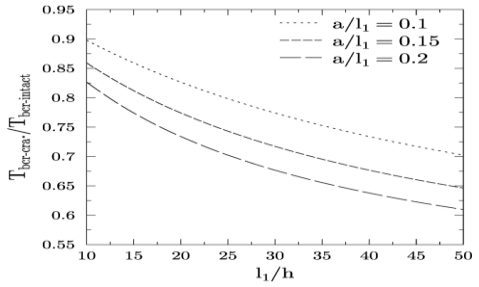

Fig.8
Variation of non-dimensional critical buckling temperature with l_1 / h for various crack lengths, $l_1 / l_2 = 1$.

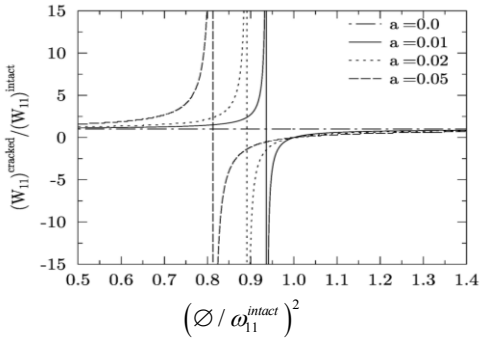

Fig.9
Central deflection ratio $W_{11}^{cracked} / W_{11}^{intact}$ versus the normalized operational frequency $\left(\varnothing / \omega_{11}^{intact}\right)^2$ for various values of crack length (a).

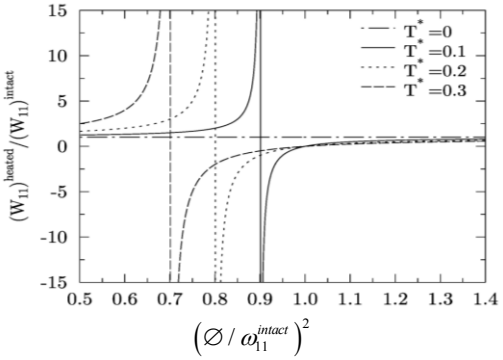

Fig.10
Central deflection ratio $W_{11}^{heated} / W_{11}^{intact}$ versus the normalized operational frequency $\left(\varnothing / \omega_{11}^{intact}\right)^2$ for various values of temperature (T^*).

7 CONCLUSIONS

In the present study, an attempt has been made to develop an analytical model for free vibration analysis of a partially cracked magneto-electro-elastic (MEE) plate subjected to thermal environment. The proposed model is capable of predicting the vibration response of cracked magneto-electro-thermo-elastic plate and has obvious advantage of being simple, efficient computation time and ease of parametric study. The classical governing equation is thoroughly modified to accommodate the effect of pyroelectric and pyromagnetic behavior on free

vibration of MEE plate. The analytical results obtained from present study shows the influence of crack length, plate aspect ratio and rise in temperature on fundamental frequency of MEE plate. It is established that the fundamental frequency is decreased by rise in temperature of the plate and this decrease in frequency is further augmented by presence of a partial crack. A unique classical expression for buckling temperature of cracked magneto-electro-thermo-elastic plate is presented discounting geometric nonlinearity. It is shown that the presence of the crack at the centre of plate decreases the critical buckling temperature. The fact that the natural frequency and critical buckling temperature for an intact plate decreases with increase in plate aspect ratio is established to be true for cracked MEE plate also. A classical relation for central deflection of cracked and heated MEE plate is also proposed. The effect of varying forcing frequency, crack length and temperature rise on deflection has been established. To the best of the authors' knowledge, this is the first attempt to model vibrations of a cracked magneto-electro-thermo-elastic plate subjected to temperature rise and hence it would be instructive to formulate the model using some shear deformation theory or FEM technique.

REFERENCES

[1] Chang T.P., 2013, On the natural frequency of transversely isotropic magneto-electro-elastic plates in contact with fluid, *Applied Mathematical Modelling* **37**: 2503-2515.

[2] Liu M., 2011, An exact deformation analysis for the magneto-electro-elastic fiber-reinforced thin plate, *Applied Mathematical Modelling* **35**: 2443-2461.

[3] Liu M., Chang T., 2010, Closed form expression for the vibration problem of a transversely isotropic magneto-electro-elastic plate, *Journal of Applied Mechanics* **77**: 1-8.

[4] Chen Z., Yu S., Meng L., Lin Y., 2006, Effective properties of layered magneto-electro-elastic composites, *Composite Structures* **57**: 177-182.

[5] Li J.Y., 2000, Magnetoelectroelastic multi-inclusion and inhomogeneity problems and their applications in composite materials, *International Journal* of *Engineering Science* **38**: 1993-2011.

[6] Xue C.-X., Pan E., 2013, On the longitudinal wave along a functionally graded magneto-electro-elastic rod, *International Journal* of *Engineering Science* **62**: 48-55.

[7] Wu T.-L., Huang J.H., 2000, Closed-form solutions for the magnetoelectric coupling coefficients in fibrous composites with piezoelectric and piezomagnetic phases, *International Journal* of *Solids* and *Structures* **37**: 2981-3009.

[8] Pan E., 2001, Exact solution for simply supported and multilayered magneto-electro-elastic plates, *Journal of Applied Mechanics* **68**: 608.

[9] Pan E., Heyliger P.R., 2002, Free vibrations of simply supported and multilayered magneto-electro-elastic plates, *Journal of Sound and Vibration* **252**: 429-442.

[10] Ramirez F., Heyliger P.R., Pan E., 2006, Free vibration response of two-dimensional magneto-electro-elastic laminated plates, *Journal of Sound and Vibration* **292**: 626-644.

[11] Ramirez F., Heyliger P.R., Pan E., 2006, Discrete layer solution to free vibrations of functionally graded magneto-electro-elastic plates, *Mechanics of Advanced Materials and Structures* **13**: 249-266.

[12] Simões Moita J.M., Mota Soares C.M., Mota Soares C.A., 2009, Analyses of magneto-electro-elastic plates using a higher order finite element model, *Composite Structures* **91**: 421-426.

[13] Milazzo A., 2012, An equivalent single-layer model for magnetoelectroelastic multilayered plate dynamics, *Composite Structures* **94**: 2078-2086.

[14] Milazzo A., 2014, Layer-wise and equivalent single layer models for smart multilayered plates, *Composites Part B: Engineering* **67**: 62-75.

[15] Milazzo A., 2014, Refined equivalent single layer formulations and finite elements for smart laminates free vibrations, *Composites Part B: Engineering* **61**: 238-253.

[16] Kattimani S.C., Ray M.C., 2015, Control of geometrically nonlinear vibrations of functionally graded magneto-electro-elastic plates, *International Journal of Mechanical Sciences* **99**: 154-167.

[17] Li Y., Zhang J.,2014, Free vibration analysis of magnetoelectroelastic plate resting on a Pasternak foundation, *Smart Materials and Structures* **23**: 25002.

[18] Razavi S., Shooshtari A., 2015, Nonlinear free vibration of magneto-electro-elastic rectangular plates, *Composite Structures* **119**: 377-384.

[19] Shooshtari A., Razavi S., 2014, Nonlinear free and forced vibrations of anti-symmetric angle-ply hybrid laminated rectangular plates, *Journal of Composite Materials* **48**: 1091-1111.

[20] Shooshtari A., Razavi S., 2015, Nonlinear vibration analysis of rectangular magneto-electro-elastic thin plates, *International Journal of Engineering* **28**: 136-144.

[21] Phoenix S.S., Satsangi S.K., Singh B.N., 2009, Layer-wise modelling of magneto-electro-elastic plates, *Journal of Sound and Vibration* **324**: 798-815.

[22] Guan Q., He S.R., 2006,Three-dimensional analysis of piezoelectric/piezomagnetic elastic media, *Composite Structures* **72**: 419-428.

[23] Shooshtari A., Razavi S., 2016,Vibration analysis of a magnetoelectroelastic rectangular plate based on a higher-order shear deformation theory, *Latin American Journal of Solids and Structures* **13**: 554-572.
[24] Rao S.S., Sunar M., 1993, Analysis of distributed thermopiezoelectric sensors and actuators in advanced intelligent structures, *AIAA Journal* **31**: 1280-1284.
[25] Dunn J.Y., Dunn M.L., 1998, Anisotropic coupled field inclusion and inhomogeneity problem, *Philosophical Magazine A* **77**: 1341-1350.
[26] Li J.Y., 2003, Uniqueness and reciprocity theorems for linear thermo-electro-magneto-elasticity, *Journal of Mechanics and Applied Mathematics* **56**: 35-43.
[27] Chen W.Q., Lee K.Y., Ding H.J., 2005, On free vibration of non-homogeneous transversely isotropic magneto-electro-elastic plates, *Journal of Sound and Vibration* **279**: 237-251.
[28] Hou P.F., Leung A.Y., Ding H.J., 2008, A point heat source on the surface of a semi-infinite transversely isotropic electro-magneto-thermo-elastic material, *International Journal* of *Engineering Science* **46**: 273-285.
[29] Hou P.F., Teng G.H., Chen H.R., 2009,Three-dimensional Green's function for a point heat source in two-phase transversely isotropic magneto-electro-thermo-elastic material, *Mechanics of Materials* **41**: 329-338.
[30] Ke L.L., Wang Y.S., Yang J., Kitipornchai S., 2014, Free vibration of size-dependent magneto-electro-elastic nanoplates based on the nonlocal theory, *Acta Mechanica Sinica/Lixue Xuebao* **30**: 516-525.
[31] Rice J., Levy N., 1972, The part-through surface crack in an elastic plate, *Journal of Applied Mechanics* **39**(1): 185-194.
[32] Delale F., Erdogan F., 1981, Line-spring model for surface cracks in a reissner plate, *International Journal* of *Engineering Science* **19**: 1331-1340.
[33] Zheng Z., Dai S., 1994, Stress intensity factors for an inclined surface crack under biaxial, *Engineering Fracture Mechanics* **47**: 281-289.
[34] Khadem S.E., Rezaee M., 2000, Introduction of modified comparison functions for vibration analysis of a rectangular cracked plate, *Journal of Sound and Vibration* **236**: 245-258.
[35] Israr A., Cartmell M.P., Manoach E., Trendafilova I., Ostachowicz W., Krawczuk M., Zak A., 2009, Analytical modelling and vibration analysis of cracked rectangular plates with different loading and boundary conditions, *Journal of Applied Mechanics* **76**: 1-9.
[36] Ismail R., Cartmell M.P., 2012, An investigation into the vibration analysis of a plate with a surface crack of variable angular orientation, *Journal of Sound and Vibration* **331**: 2929-2948.
[37] Joshi P.V., Jain N.K., Ramtekkar G.D., 2014, Analytical modeling and vibration analysis of internally cracked rectangular plates, *Journal of Sound and Vibration* **333**: 5851-5864.
[38] Joshi P. V., Jain N.K., Ramtekkar G.D., 2015, Analytical modelling for vibration analysis of partially cracked orthotropic rectangular plates, *European Journal of Mechanics - A/Solids* **50**: 100-111.
[39] Gupta A., Jain N.K., Salhotra R., Joshi P.V., 2015, Effect of microstructure on vibration characteristics of partially cracked rectangular plates based on a modified couple stress theory, *International Journal* of *Engineering Science* **100**: 269-282.
[40] Gupta A., Jain N.K., Salhotra R., Rawani A.M., Joshi P.V., 2015, Effect of fibre orientation on non-linear vibration of partially cracked thin rectangular orthotropic micro plate: An analytical approach, *International Journal* of *Engineering Science* **105**: 378-397.
[41] Joshi P. V., Jain N.K., Ramtekkar G.D., 2015, Effect of thermal environment on free vibration of cracked rectangular plate: An analytical approach, *Thin-Walled Structures* **91**: 38-49.
[42] Joshi P.V., Jain N.K., Ramtekkar G.D., Singh Virdi G., 2016, Vibration and buckling analysis of partially cracked thin orthotropic rectangular plates in thermal environment, *Thin-Walled Structures* **109**: 143-158.
[43] Soni S., Jain N.K., Joshi P. V., 2017, Analytical modeling for nonlinear vibration analysis of partially cracked thin magneto-electro-elastic plate coupled with fluid, *Nonlinear Dynamics* **90**: 137-170.
[44] Kondaiah P., Shankar K., Ganesan N., 2012, Studies on magneto-electro-elastic cantilever beam under thermal environment, *Coupled Systems Mechanics* **1**: 205-217.
[45] Zhang C.L., 2013, Discussion : Closed form expression for the vibration problem of a transversely isotropic, *Journal of Applied Mechanics* **80**: 15501.
[46] Gao C., Noda N., 2004, Thermal-induced interfacial cracking of magnetoelectroelastic materials, *International Journal* of *Engineering Science* **42**: 1347-1360.
[47] Berger H., 1954, *A New Approach to the Analysis of Large Deflections of Plates*, Dissertation (Ph.D.), California Institute of Technology.
[48] Szilard R., 2004, *Theories and Applications of Plate Analysis*, John Wiley & Sons, Inc., Hoboken, NJ, USA.
[49] Jones R.M., 2006, *Buckling of Bars, Plates, and Shells*, Bull Ridge Corporation.
[50] Ventsel E., Krauthammer T., Carrera E., 2002, *Thin Plates and Shells: Theory, Analysis, and Applications*, CRC Press.
[51] Murphy K.D., Virgin L.N., Rizzi S.A., 1997, The effect of thermal prestress on the free vibration characteristics of clamped rectangular plates: Theory and experiment, *Journal of Vibration and Acoustics* **119**: 243.
[52] Huang C.S., Leissa A.W., Chan C.W., 2011, Vibrations of rectangular plates with internal cracks or slits *International Journal* of *Engineering Science* **53**: 436-445.
[53] Bose T., Mohanty A.R., 2013, Vibration analysis of a rectangular thin isotropic plate with a part-through surface crack of arbitrary orientation and position, *Journal of Sound and Vibration* **332**: 7123-7141.